Statistical analysis

Data were expressed as mean±SEM. Input/output function data of the amplitudes were analyzed via a non-repeated measures analysis of variance (ANOVA). The significance of DPOAE amplitudes was analyzed further by post hoc multiple comparison tests using the Bonferroni procedure. The statistical difference of DPOAE threshold was determined by a two-sided Mann–Whitney's *U*-test. $P<0.05$ was accepted as the level of significance.

RESULTS

Distortion product otoacoustic emission

DPOAE responses were examined during postnatal development. Non-transgenic mice started to show a measurable response of DPOAE from P12–14 followed by gradual increase of amplitude (Fig. 1A, B, C). Significant differ-

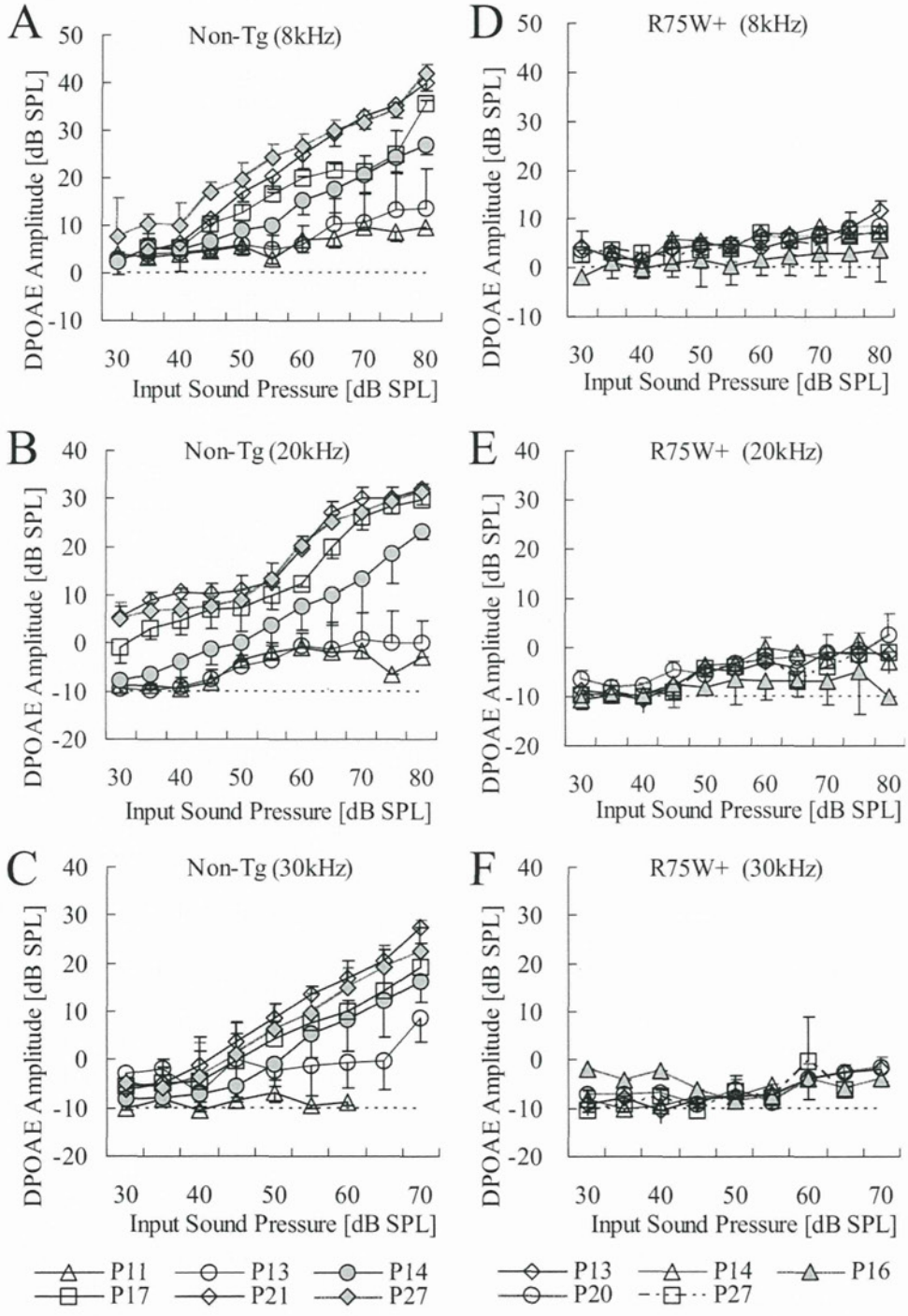

Fig. 1. Input/output function of the amplitudes of non-transgenic (A, B, C) and R75W transgenic (D, E, F) mice at 8 kHz, 20 kHz and 30 kHz frequencies (2f1–f2) from P11 to P27. DPOAE data were plotted as mean±SEM. The dotted line is the noise level. Non-Tg: non-transgenic mice, R75W+: R75W transgenic mice.

Please cite this article in press as: Minekawa A, et al., Cochlear outer hair cells in a dominant-negative connexin26 mutant mouse preserve non-linear capacitance in spite of impaired distortion product otoacoustic emission, Neuroscience (2009), doi: 10.1016/j.neuroscience.2009.08.043

ences of the DPOAE amplitudes of the non-transgenic mice in comparison to noise levels appeared at P12–14 for the different stimuli tested. In contrast, there were no statistically significant differences between noise level and DPOAE amplitudes at 8 kHz, 20 kHz, and 30 kHz throughout postnatal development in the R75W transgenic mice. Furthermore, no DPOAE was detected at any frequencies in R75W transgenic mice throughout postnatal development (Fig. 1D, E, F).

The mean DPOAE thresholds of non-transgenic mice were abruptly reduced around P13–P14 to reach the adult level by P16. In contrast, the mean DOPAE thresholds of R75W transgenic mice stayed at high level throughout postnatal development (Fig. 2).

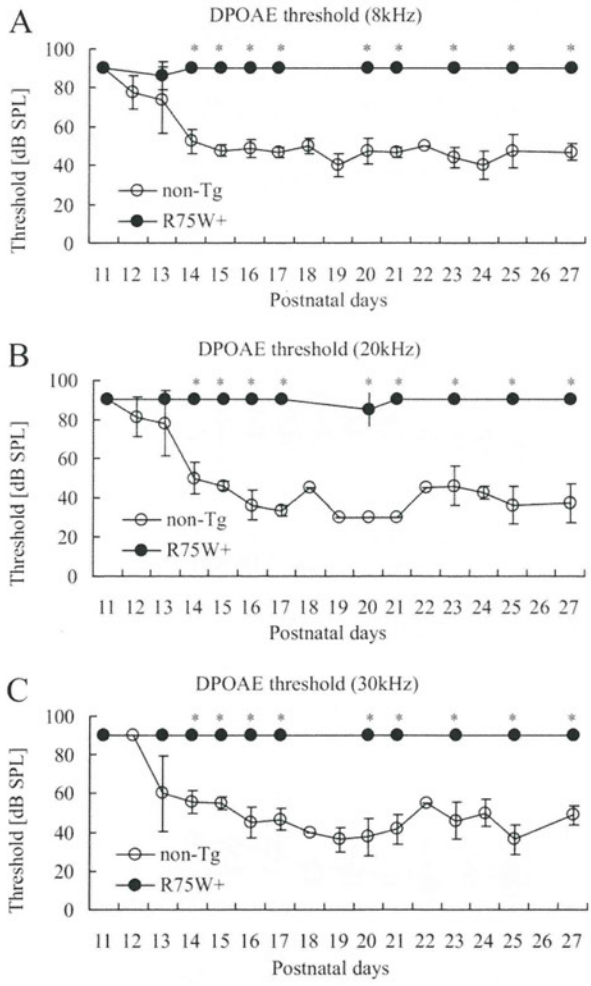

Fig. 2. DPOAE thresholds at 8 kHz (A), 20 kHz (B), and 30 kHz (C) frequencies of non-transgenic mice (open circle) and R75W transgenic mice (filled circle) from P11 to P27. The DPOAE threshold level was defined as the dB level at which the 2f1–f2 distortion product was more than 10 dB above the noise level. In the case of no DPOAE, the threshold level was defined as 90 dB. *: Significant difference between non-transgenic and transgenic mice ($P<0.05$). Non-Tg: non-transgenic mice, R75W+: R75W transgenic mice.

Histology and immunohistochemistry

The cytoarchitecture of the organ of Corti of the R75W transgenic mouse was remarkably different from that of the non-transgenic mouse (Fig. 3A, B). Transverse sections of the organ of Corti in R75W transgenic mouse revealed compression and squeezing of the OHC by the surrounding supporting cells, and Nuel's space around each OHC was occupied by Deiter's cells (Fig. 3B). Structural changes in the OHCs and adjacent cells are likely to restrict the electrically-induced motility of the OHC. The mesothelial cells associated with the basilar membrane in the transgenic mouse were cuboidal and more densely packed in contrast to a flattened layer in the control mouse. However, the ultrastructure of the OHCs in the non-transgenic mouse was comparable to that of the R75W transgenic mouse (Fig. 3C, D). The OHC of both mice showed consistent characteristic features; (i) a relatively high proportion of cytoplasm having a basally located nucleus, (ii) a smooth plasma membrane lined by a thick layer of subsurface cisternae, (iii) numerous mitochondria along the lateral membrane, and (iv) no vacuole formation in the cytoplasm and no condensation of chromatin in the nucleus.

Immunofluorescence microscopy of cross-cochlear sections was used to examine the distribution of prestin in the apical turns of the cochlea of non-transgenic and R75W transgenic mice at P12. Prestin labeling was clearly visible on the whole OHC basolateral wall in both the control (Fig. 4A) and R75W+ mice (Fig. 4B) at P12. On the other hand, the nucleus and the cuticular plate of both mice were devoid of immunostaining.

These ultrastructural and immunohistochemical results support the notion that the OHC are equipped with the morphological and molecular bases to produce electromotility.

Electromotility of OHCs

The signature electrical response of an adult OHC is a bell-shaped, voltage-dependent capacitance, which represents the conformational fluctuations of the motor molecule. In wild-type of C57BL/6J mice, *Cv* increased rapidly during development, saturating at P18 (Abe et al., 2007). OHCs from both R75W transgenic and non-transgenic mice showed somatic shape change in response to the voltage change (data not shown) and showed a typical bell-shaped voltage dependence (Fig. 5A). *Cv* increased progressively from P9 and saturated at P24. The time course of *Cv* in R75W transgenic and non-transgenic mice showed no significant difference (Fig. 5B). These results indicate that the development of OHC motility is not affected in R75W transgenic mice.

DISCUSSION

The present study demonstrated that a dominant-negative R75W mutation of *Gjb2* failed to generate a detectable DPOAE from birth in spite of the presence of OHCs and apparently normal electromotility. The DPOAE depends on two factors, an intact OHC system (Long and Tubis, 1988; Brown et al., 1989) and a positive endocochlear potential

Please cite this article in press as: Minekawa A, et al., Cochlear outer hair cells in a dominant-negative connexin26 mutant mouse preserve non-linear capacitance in spite of impaired distortion product otoacoustic emission, Neuroscience (2009), doi: 10.1016/j.neuroscience.2009.08.043

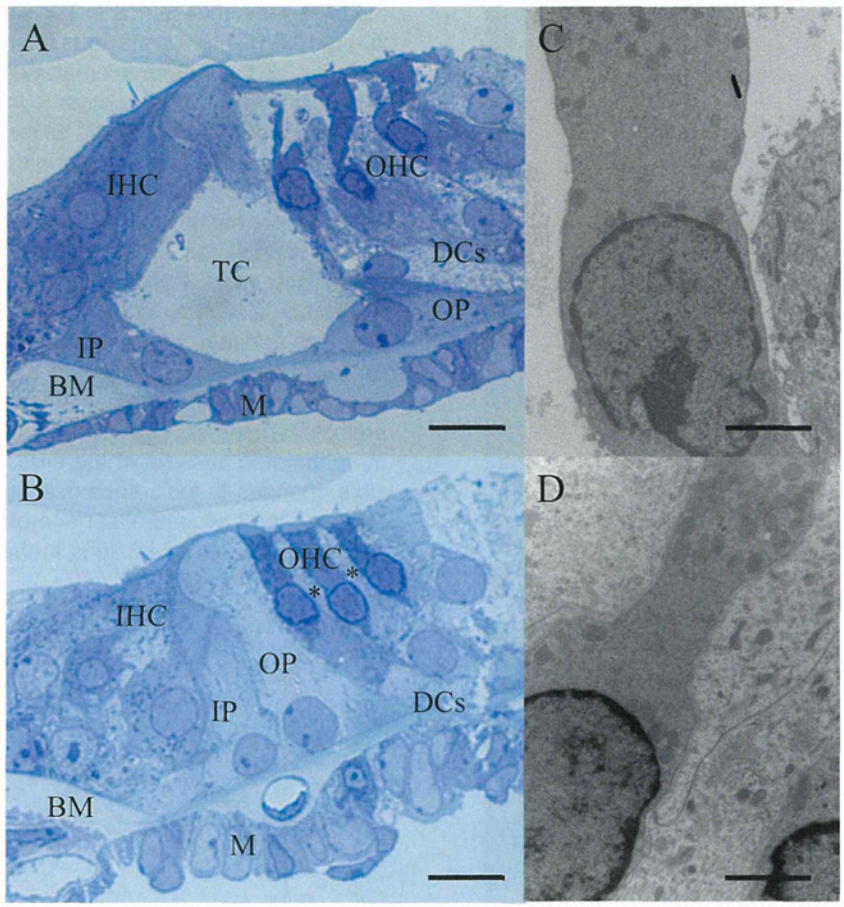

Fig. 3. Histology and transmission electron micrographs of non-transgenic (A, C) and R75W transgenic (B, D) mice. At P12, tunnel of Corti is detected in non-transgenic mice (A), but not (asterisk) in R75W transgenic mice (B). Nuel's space is formed in non-transgenic mice (A, C), but not in R75W transgenic mice (B, D). OHCs are detected in both non-transgenic (A) and R75W transgenic mice, but are squeezed by the surrounding Deiter's in R75W transgenic mice (B). The OHCs showed normal development, with preserved fine structure of the lateral wall, membrane-bound subsurface cisterna beneath the plasma membrane, and enriched mitochondria in both the non-transgenic (C) and R75W transgenic mice (D). Scale bars are 10 μm (A, B) and 2 μm (C, D). Abbreviations used: TC, tunnel of Corti; IP, inner pillar cell; OP, outer pillar cell; BM, basilar membrane; M, mesothelial cell.

(Brownell, 1990). The R75W transgenic mice have a normal endocochlear potential (Kudo et al., 2003). Furthermore, the OHC develops normally with apparently intact fine structure of the lateral wall, including normal membrane-bound subsurface cisterna beneath the plasma membrane. The characteristic phenotype observed in the R75W transgenic mice was the absence of the tunnel of Corti, Nuel's space, and spaces surrounding the OHC, related to abnormal development of the supporting cells.

The mammalian cochlea uses a unique mechanism for amplification of sound signals. Cochlear amplification is thought to originate from (1) somatic motility based on the cochlear motor prestin and (2) hair cell bundle motor related to mechanoelectrical channel (Robles and Ruggero, 2002). Distortion and cochlear amplification are believed to stem from a common mechanism. A recent study (Verpy et al., 2008) postulated that the main source of cochlear waveform distortions is a deflection-dependent hair bundle stiffness derived from stereocilin associated with the horizontal top connectors. However, the relationship between stereocilin and prestin is still unclear.

Somatic electromotility of the OHC is a voltage-dependent rapid alteration of OHC length and stiffness. The electromotility of the OHC is thought to amplify the motion of the basilar membrane at low sound pressure levels and compress it at high levels (Patuzzi et al., 1989; Ruggero and Rich, 1991; Kossl and Russell, 1992). Prestin, which resides in the basolateral membrane of the cochlear OHC (Yu et al., 2006), acts as a voltage-dependent motor protein responsible for OHC electromotility (Belyantseva et al., 2000; Zheng et al., 2000; Liberman et al., 2002). The present study demonstrated that the voltage-dependent, nonlinear capacitance representing the conformational fluctuations of the motor molecule progressively increased from P10 to P18 in *Gjb2* R75W transgenic mice. The developmental changes in the OHC electromotility observed in the *Gjb2* R75W transgenic mice resemble those of both the C57BL/6J mouse in a previous study (Abe et al., 2007) and the littermate non-transgenic mice in the present study.

At least three factors that could explain the discrepancy between the DPOAE and the OHC electromotility

Please cite this article in press as: Minekawa A, et al., Cochlear outer hair cells in a dominant-negative connexin26 mutant mouse preserve non-linear capacitance in spite of impaired distortion product otoacoustic emission, Neuroscience (2009), doi: 10.1016/j.neuroscience.2009.08.043

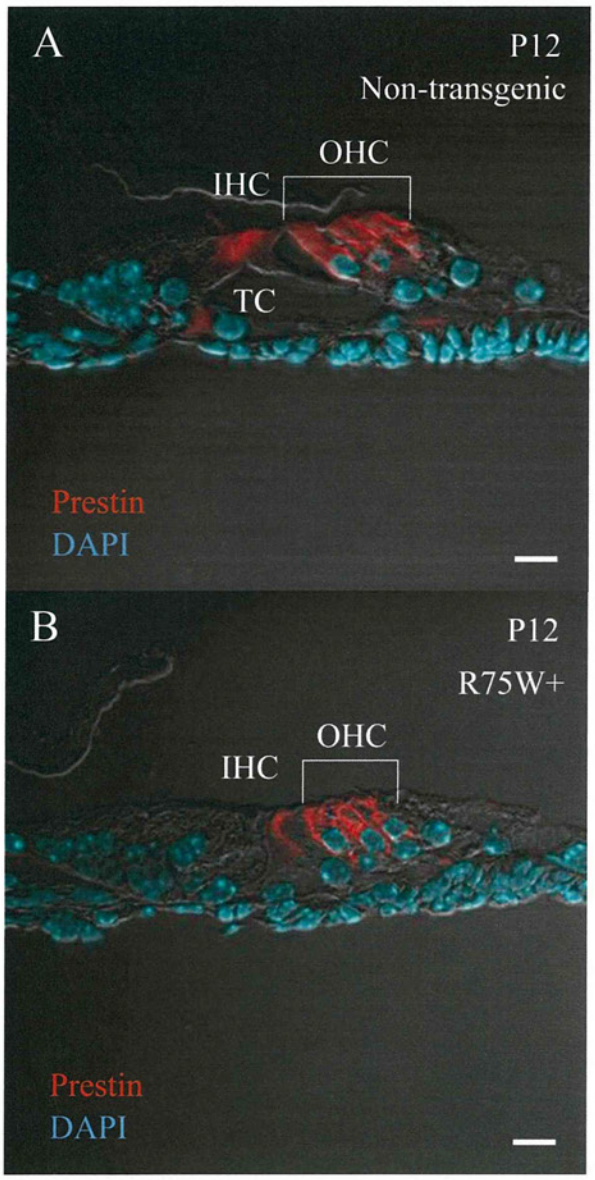

Fig. 4. A cross-sectional immunofluorescent analysis of prestin distributed in the apical turns of the cochlea of non-transgenic (A) and R75W transgenic mice (B) at P12. Prestin labeling (red) is clearly visible on the whole OHC basolateral wall in both the non-transgenic (A) and R75W transgenic mice (B) at P12. The extracellular space around the OHC in R75W transgenic mice is narrower than that in non-transgenic mice. On the other hand, the nucleus stained with DAPI (blue) and the cuticular plate of both mice are devoid of immunostaining. Abbreviations used: OHC, outer hair cell; IHC, inner hair cell. Scale bars are 10 μm (A, B).

arising from the failure of development of the supporting cells can be proposed. First, mature OHCs are supported by underlying Deiter's cells, flanked on the lateral edge by a several rows of Hensen's cells, and anchored by the reticular lamina at their apical surface. The three-dimensional structure of the OHCs enable the longitudinal changes driven by transmembrane potential changes. In the transgenic mouse, the OHCs were compressed by the surrounding Deiter's cells, thus restricting motility. Second, vibration of the basilar membrane may be related to its thickness, which would contribute to the sensitivity and the production of the otoacoustic emissions (Kossl and Vater, 1985) and further to the tonotopic changes of the developing gerbil cochlea (Schweitzer et al., 1996). The thickened basilar membrane observed in the transgenic mice might suppress the DPOAE by reducing the basilar membrane vibration. Structural changes in the basilar membrane may also reduce the sound-induced vibration of the cochlear partition, thus inhibiting deflection of stereocilia on inner hair cells. This could explain why *Gjb2* R75W transgenic mice show remarkable elevation of the auditory brainstem response threshold (Inoshita et al., 2008). Third, morphometric analysis of the organ of Corti suggest possible changes in ionic composition of the cortilymph surrounding the basolateral surface of the OHCs (Inoshita et al., 2008). Increased K^+ ions in the cortilymph would de-

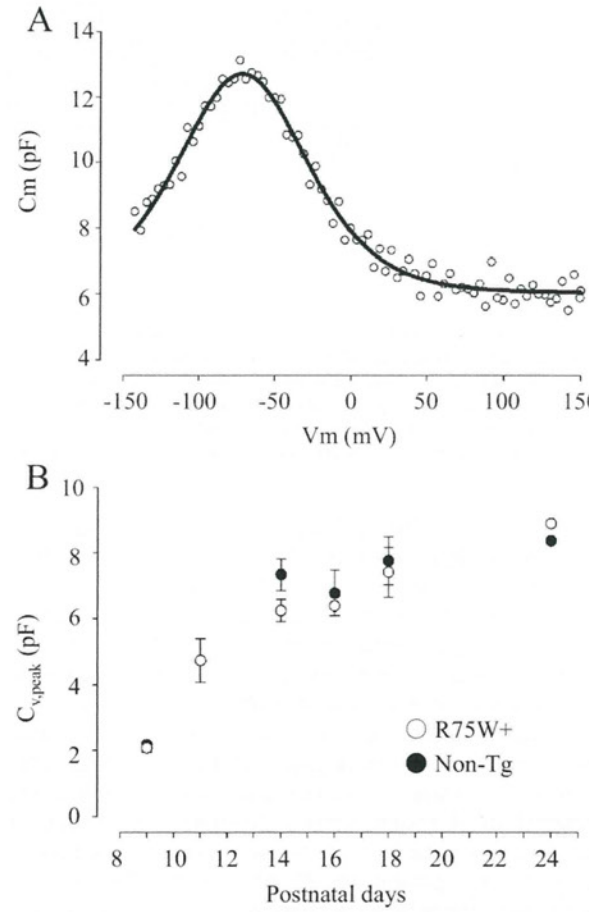

Fig. 5. Electrical responses of isolated OHC. C_m is expressed as a function of V_m at P14 in the R75W transgenic mouse (A). Fitted parameters are Q_{max}=0.704 pC, z=0.89. C_v, peak is expressed as a function of postnatal day (B). The number of cells in non-transgenic (closed circle) and R75W transgenic mice (open circle) was (from P9 to P24) 1–2, 0–3, 2–3, 5–2, 3–3, and 1–1, respectively. Standard error is plotted. Non-Tg: non-transgenic mice, R75W+: R75W transgenic mice.

Please cite this article in press as: Minekawa A, et al., Cochlear outer hair cells in a dominant-negative connexin26 mutant mouse preserve non-linear capacitance in spite of impaired distortion product otoacoustic emission, Neuroscience (2009), doi: 10.1016/j.neuroscience.2009.08.043

polarize the OHCs, and decreased driving force across the mechanosensitive channels could affect OHC electromotility. The progressive degeneration of OHCs observed in the adult R75W transgenic mice (Kudo et al., 2003) may be brought about by disturbed homeostasis of the cortilymph.

The secondary hair cell loss in adult R75W transgenic mice (Kudo et al., 2003; Inoshita et al., 2008) implies that the restoration of hearing requires the regeneration of hair cells in addition to introduction of the *Gjb2* gene. The present study clearly showed both morphological and functional maturation of OHC until late in development, suggesting that a dominant-negative R75W mutation of *Gjb2* does not affect the genes that determine or control the differentiation of the OHC. Therefore, gene transfer of *Gjb2* into the supporting cells before hair cell degeneration could be used to treat deafness. Transgene expression has been accomplished in the supporting cells of the neonatal mouse cochlea using adeno-associated viral vectors without causing additional damage to the cochlea (Iizuka et al., 2008). Therefore, the present study provides a new strategy to restore hearing in *Gjb2*-based mutation.

CONCLUSION

OHC from the dominant-negative R75W mutation of *Gjb2* showed normal development and maturation, and isolated OHC clearly showed voltage-dependent, nonlinear capacitance with characteristic subcellular features. However, the DPOAE, which serves as an index for *in vivo* cochlear amplification, was remarkably suppressed in the mutant mice. This may result from disturbed development of the supporting cells surrounding the OHCs. The present study confirmed that the normal development of the supporting cells is indispensable for the cellular function of the OHC.

REFERENCES

Abe T, Kakehata S, Kitani R, Maruya S, Navaratnam D, Santos-Sacchi J, Shinkawa H (2007) Developmental expression of the outer hair cell motor prestin in the mouse. J Membr Biol 215:49–56.

Beltramello M, Piazza V, Bukauskas FF, Pozzan T, Mammano F (2005) Impaired permeability to Ins(1,4,5)P3 in a mutant connexin underlies recessive hereditary deafness. Nat Cell Biol 7: 63–69.

Belyantseva IA, Adler HJ, Curi R, Frolenkov GI, Kachar B (2000) Expression and localization of prestin and the sugar transporter GLUT-5 during development of electromotility in cochlear outer hair cells. J Neurosci 20:RC116.

Brown AM, McDowell B, Forge A (1989) Acoustic distortion products can be used to monitor the effects of chronic gentamicin treatment. Hear Res 42:143–156.

Brownell WE (1990) Outer hair cell electromotility and otoacoustic emissions. Ear Hear 11:82–92.

Cohen-Salmon M, Ott T, Michel V, Hardelin JP, Perfettini I, Eybalin M, Wu T, Marcus DC, Wangemann P, Willecke K, Petit C (2002) Targeted ablation of connexin26 in the inner ear epithelial gap junction network causes hearing impairment and cell death. Curr Biol 12:1106–1111.

Colvin JS, Bohne BA, Harding GW, McEwen DG, Ornitz DM (1996) Skeletal overgrowth and deafness in mice lacking fibroblast growth factor receptor 3. Nat Genet 12:390–397.

Forge A, Becker D, Casalotti S, Edwards J, Marziano N, Nevill G (2003) Gap junctions in the inner ear: comparison of distribution patterns in different vertebrates and assessement of connexin composition in mammals. J Comp Neurol 467:207–231.

Gossman DG, Zhao HB (2008) Hemichannel-mediated inositol 1,4,5-trisphosphate (IP3) release in the cochlea: a novel mechanism of IP3 intercellular signaling. Cell Commun Adhes 15: 305–315.

Iizuka T, Kanzaki S, Mochizuki H, Inoshita A, Narui Y, Furukawa M, Kusunoki T, Saji M, Ogawa K, Ikeda K (2008) Noninvasive in vivo delivery of transgene via adeno-associated virus into supporting cells of the neonatal mouse cochlea. Hum Gene Ther 19:384–390.

Inoshita A, Iizuka T, Okamura HO, Minekawa A, Kojima K, Furukawa M, Kusunoki T, Ikeda K (2008) Postnatal development of the organ of Corti in dominant-negative Gjb2 transgenic mice. Neuroscience 156:1039–1047.

Kikuchi T, Kimura RS, Paul DL, Adams JC (1995) Gap junctions in the rat cochlea: immunohistochemical and ultrastructural analysis. Anat Embryol (Berl) 191:101–118.

Kitsunai Y, Yoshida N, Murakoshi M, Iida K, Kumano S, Kobayashi T, Wada H (2007) Effects of heat stress on filamentous actin and prestin of outer hair cells in mice. Brain Res 1177:47–58.

Kossl M, Russell IJ (1992) The phase and magnitude of hair cell receptor potentials and frequency tuning in the guinea pig cochlea. J Neurosci 12:1575–1586.

Kossl M, Vater M (1985) Evoked acoustic emissions and cochlear microphonics in the mustache bat, Pteronotus parnellii. Hear Res 19:157–170.

Kudo T, Kure S, Ikeda K, Xia AP, Katori Y, Suzuki M, Kojima K, Ichinohe A, Suzuki Y, Aoki Y, Kobayashi T, Matsubara Y (2003) Transgenic expression of a dominant-negative connexin26 causes degeneration of the organ of Corti and non-syndromic deafness. Hum Mol Genet 12:995–1004.

Liberman MC, Gao J, He DZ, Wu X, Jia S, Zuo J (2002) Pressing is required for electromotility of the outer hair cell and for the cochlear amplifier. Nature 419:300–304.

Long GR, Tubis A (1988) Investigations into the nature of the association between threshold microstructure and otoacoustic emissions. Hear Res 36:125–138.

Narui Y, Minekawa A, Iizuka T, Furukawa M, Kusunoki T, Koike T, Ikeda K (2009) Development of distortion product otoacoustic emissions in C57BL/6J mice. Int J Audiol 48:576–581.

Patuzzi RB, Yates GK, Johnstone BM (1989) Outer hair cell receptor current and sensorineural hearing loss. Hear Res 42:47–72.

Piazza V, Ciubotaru CD, Gale JE, Mammano F (2007) Purinergic signalling and intercellular Ca2+ wave propagation in the organ of Corti. Cell Calcium 41:77–86.

Robles L, Ruggero MA (2002) Mechanics of the mammalian cochlea. Physiol Rev 81:1305–1352.

Ruggero MA, Rich NC (1991) Furosemide alters organ of corti mechanics: evidence for feedback of outer hair cells upon the basilar membrane. J Neurosci 11:1057–1067.

Santos-Sacchi J (1991) Reversible inhibition of voltage-dependent outer hair cell motility and capacitance. J Neurosci 11:3096–3110.

Santos-Sacchi J (2004) Determination of cell capacitance using the exact empirical solution of partial differential Y/partial differential Cm and its phase angle. Biophys J 87:714–727.

Santos-Sacchi J, Kakehata S, Takahashi S (1998) Effects of membrane potential on the voltage dependence of motility-related charge in outer hair cells of the guinea-pig. J Physiol 510: 225–235.

Schweitzer L, Lutz C, Hobbs M, Weaver SP (1996) Anatomical correlates of the passive properties underlying the developmental shift in the frequency map of the mammalian cochlea. Hear Res 97:84–94.

Please cite this article in press as: Minekawa A, et al., Cochlear outer hair cells in a dominant-negative connexin26 mutant mouse preserve non-linear capacitance in spite of impaired distortion product otoacoustic emission, Neuroscience (2009), doi: 10.1016/j.neuroscience.2009.08.043

Tritsch NX, Yi E, Gale JE, Glowatzki E, Bergles DE (2007) The origin of spontaneous activity in the developing auditory system. Nature 450:50–55.

Verpy E, Weil D, Leibovici M, Goodyear RJ, Hamard G, Houdon C, Lefèvre GM, Hardelin JP, Richardson GP, Avan P, Petit C (2008) Stereocilin-deficient mice reveal the origin of cochlear waveform distortions. Nature 456:255–258.

Yu N, Zhu ML, Zhao HB (2006) Prestin is expressed on the whole outer hair cell basolateral surface. Brain Res 1095:51–58.

Zhao HB, Yu N, Fleming CR (2005) Gap junctional hemichannel-mediated ATP release and hearing controls in the inner ear. Proc Natl Acad Sci U S A 102:18724–18729.

Zhao HB, Yu N (2006) Distinct and gradient distributions of connexin26 and connexin30 in the cochlear sensory epithelium of guinea pigs. J Comp Neurol 499:506–518.

Zheng J, Shen W, He DZ, Long KB, Madison LD, Dallos P (2000) Prestin is the motor protein of cochlear outer hair cells. Nature 405:149–155.

(Accepted 19 August 2009)

Please cite this article in press as: Minekawa A, et al., Cochlear outer hair cells in a dominant-negative connexin26 mutant mouse preserve non-linear capacitance in spite of impaired distortion product otoacoustic emission, Neuroscience (2009), doi: 10.1016/j.neuroscience.2009.08.043

Otol Jpn 19(3):214-218, 2009　第18回日本耳科学会総会シンポジウム「血管条とラセン靱帯機能の新しい展開」特集

←前号に続く

3．Cell therapy targeting cochlear fibrocytes

神谷　和作
順天堂大学医学部耳鼻咽喉科学教室

Cell therapy targeting cochlear fibrocytes

Kazusaku Kamiya
Juntendo University School of Medicine, Department of Otoralyngology

Recently, a number of clinical studies for cell therapy have been reported and clinically used for several intractable diseases. Inner ear cell therapy for sensorineural hearing loss also has been studied using some laboratory animals, although the successful reports for the hearing recovery were still few.

Cochlear fibrocytes play important roles in normal hearing as well as in several types of sensorineural hearing loss due to inner ear homeostasis disorders. Recently, we developed a novel rat model of acute sensorineural hearing loss due to fibrocyte dysfunction induced by a mitochondrial toxin[1), 2)]. In this model, we demonstrate active regeneration of the cochlear fibrocytes after severe focal apoptosis without any changes in the organ of Corti. To rescue the residual hearing loss, we transplanted mesenchymal stem cells into the lateral semicircular canal; a number of these stem cells were then detected in the injured area in the lateral wall. Rats with transplanted mesenchymal stem cells in the lateral wall demonstrated a significantly higher hearing recovery ratio than controls. The mesenchymal stem cells in the lateral wall also showed connexin 26 and connexin 30 immunostaining reminiscent of gap junctions between neighboring cells[3)]. These results indicate that reorganization of the cochlear fibrocytes leads to hearing recovery after acute sensorineural hearing loss in this model and suggest that mesenchymal stem cell transplantation into the inner ear may be a promising therapy for patients with sensorineural hearing loss due to degeneration of cochlear fibrocytes.

Key words：cochlear fibrocyte, inner ear cell therapy, mesenchymal stem cell
和文キーワード：蝸牛線維細胞，内耳細胞療法，間葉系幹細胞

Mammalian cochlear fibrocytes of the mesenchymal nonsensory regions play important roles in the cochlear physiology of hearing, including the transport of potassium ions to generate an endocochlear potential in the endolymph that is essential for the transduction of sound by hair cells[4), 5), 6)]. It has been postulated that a potassium recycling pathway toward the stria vascularis via fibrocytes in the cochlear lateral wall is critical for proper hearing, although the exact mechanism has not been definitively proven[5)]. One candidate model for this ion transport system consists of an extracellular flow of potassium ions through the scala tympani and scala vestibuli and a transcellular flow through the organ of Corti, supporting cells, and cells of the lateral wall[7), 8)]. The fibrocytes within the cochlear lateral wall are divided into type I to V based on their structural features, immunostaining patterns, and general location[8)]. Type II, type IV, and type V fibrocytes resorb potassium ions from the surrounding perilymph and from outer sulcus cells via the Na, K-ATPase. The potassium ions are then transported to type I fibrocytes, strial basal cells and intermediate cells through gap junctions, and are secreted into the intrastrial space through potassium channels. The

secreted potassium ions are incorporated into marginal cells by the Na, K-ATPase and the Na-K-Cl cotransporter, and are finally secreted into the endolymph through potassium channels.

Degeneration and alteration of the cochlear fibrocytes have been reported to cause hearing loss without any other changes in the cochlea in the Pit-Oct-Unc (POU)-domain transcription factor Brain-4 (Brn-4) deficient mouse[9] and the otospiralin deficient mouse[6]. Brn-4 is the gene responsible for human DFN3 (Deafness 3), an X chromosome-linked nonsyndromic hearing loss. Mice deficient in Brn-4 exhibit reduced endocochlear potential and hearing loss and show severe ultrastructural alterations, including cellular atrophy and a reduction in the number of mitochondria, exclusively in spiral ligament fibrocytes[9), 10]. In the otospiralin deficient mouse, degeneration of type II and IV fibrocytes is the main pathological change and hair cells and the stria vascularis appear normal[6]. Furthermore, in mouse and gerbil models of age-related hearing loss[11), 12), 13], degeneration of the cochlear fibrocytes preceded the degeneration of other types of cells within the cochlea, with notable pathological changes seen especially in type II, IV, and V fibrocytes. In humans, mutations in the connexin 26 (Cx26) and connexin 30 (Cx30) genes, which encode gap junction proteins and are expressed in cochlear fibrocytes and non-sensory epithelial cells, are well known to be responsible for hereditary sensorineural deafness[14), 15]. These instances of deafness related to genetic, structural and functional alterations in the cochlear fibrocytes highlight the functional importance of these fibrocytes in maintaining normal hearing.

Generation of the animal model to study cochlear fibrocyte

To study the role of cochlear fibrocytes in hearing loss and hearing recovery, we developed an animal model of acute sensorineural hearing loss due to acute cochlear energy failure by administering the mitochondrial toxin 3-nitropropionic acid (3NP) into the rat round window niche[1), 2]. 3NP is an irreversible inhibitor of succinate dehydrogenase, a complex II enzyme of the mitochondrial electron transport chain[16), 17]. Systemic administration of 3NP has been used to produce selective striatal degeneration in the brain of several mammals[18), 19]. Our model with 3NP administration into the rat cochlea showed acute sensorineural hearing loss and revealed an initial pathological change in the fibrocytes of the lateral wall and spi-

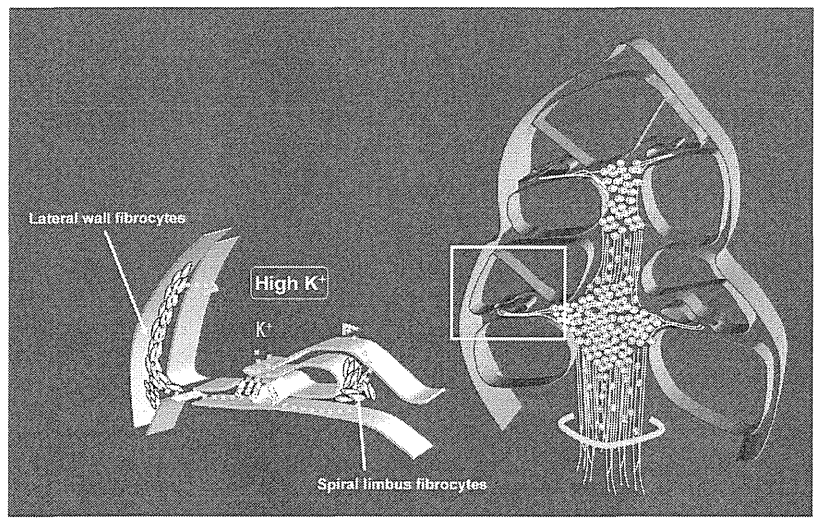

Figure. 1

The localization and the function of cochlear fibrocytes. In mammalian cochlea, ATP-dependent potassium recycling pathways have been well known as the essential mechanism for normal sound input. Cochlear fibrocytes in lateral wall and spiral limbus play a critical role in this potassium recycling system. They transport K+ into the endolymph and keep high K+ concentration mainly by Na+/K+-ATPase and gap junction.

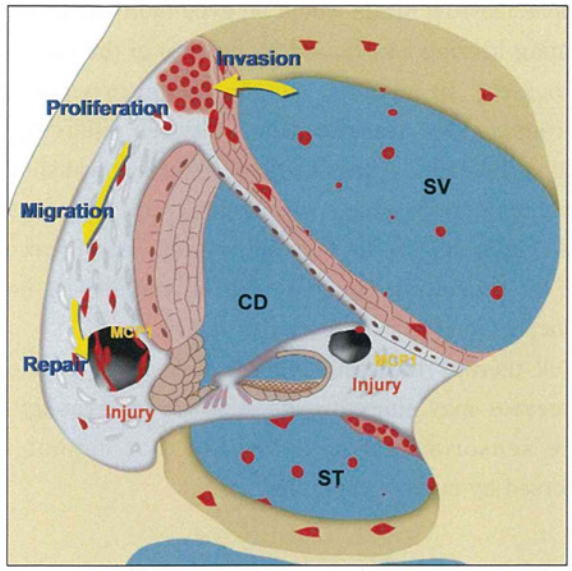

Figure. 2

A summary of the histological observations and our hypothesis for the migration of the transplanted MSCs. Arrows indicate the hypothetical route of MSC migration to the injured area. Some MSCs formed a cell mass around the scala tympani. A number of MSCs successfully invaded the lateral wall. The invading MSCs migrated and proliferated in the lateral wall. Cell migration may be induced by some chemokines such as MCP1 which was detedctd in our DNA microarray analysis. The MSCs which reached the injured area continued to proliferate and repaired the disconnected gap junction network. SV, scala vestibuli; CD, cochlear duct; ST, scala tympani. The schematic illustration was cited and modified from Am J Pathol. 171: 214-226, 2007 Kamiya, et al.

ral limbus without any significant damage to the organ of Corti or spiral ganglion. Furthermore, depending on the dose of 3NP used, these hearing loss model rats exhibited either a permanent threshold shift (PTS) or a temporary threshold shift (TTS). In the following study, we used doses of 3NP that induce TTS to explore the mechanism of hearing recovery after injury to the cochlear fibrocytes, and examined a novel therapeutic approach to repair the injured area using mesenchymal stem cell (MSC) transplantation.

Mesenchymal Stem Cell (MSC) Transplantation

MSCs are multipotent cells that can be isolated from adult bone marrow and can be induced to differentiate into a variety of tissues *in vitro* and *in vivo*[20]. Human MSCs transplanted into fetal sheep intraperitoneally undergo site-specific differentiation into chondrocytes, adipocytes, myocytes, cardiomyocytes, bone marrow stromal cells, and thymic stroma[21]. Furthermore, when MSCs were transplanted into postnatal animals, they could engraft and differentiate into several tissue-specific cell types in response to environmental cues provided by different organs[22]. These transplantability features of MSCs suggested the possibility that they could restore hearing loss in 3NP-treated rats to the normal range. Recently, experimental bone marrow transplantation into irradiated mice suggested that a part of spiral ligament which consists of cochlear fibrocytes was derived from bone marrow cells or hematopoietic stem cells[23]. This indicates that bone marrow derived stem cells such as MSC may have a capacity to repair the injury of cochlear fibrocytes.

MSC transplantation accelerated hearing recover

The 3NP-treated rats showed complete hearing recovery at low frequencies; however, there remained a residual hearing loss at higher frequencies. Considering that the cochlear fibrocytes that were injured in this model are mesenchymal in origin, we transplanted rat MSCs into the cochlea to attempt to rescue the residual hearing loss. We used MSC which we previously established and demonstrated their potential as MSC, and we further confirmed the surface antigen expression of the cells used for transplantation in flow cytometry which showed similar expression pattern to human and murine MSCs. This suggests that the cells maintained the capacity as rat MSC at the moment of transplantation. Because there is no barrier in the inner ear perilymph between the cochlear and vestibular compartments, cells delivered from the lateral semicircular canal by perilymphatic perfusion are considered to have reached the cochlea. Within the perilymph of the cochlea, these cells presumably spread through the scala vestibuli toward the apical turn of the cochlea, and then, after passing through the helicotrema where the scala vestibuli communicates with the scala tympani, kept moving through the scala tympani toward the basal turn. There is no other way in which MSCs can spread within the cochlear perilymph.

Invasion of MSC to lateral wall tissue

Our study clearly demonstrates that rat MSCs were

successfully transplanted into the inner ear of 3NP-treated rats by perilymphatic perfusion from the lateral semicircular canal. A number of MSCs were detected on the surface of the ampullary crest facing the perilymph and some of them were detected within the tissue of the ampullary crest, indicating that MSCs survived at least for 11 d after the perfusion and had maintained their ability to invade and migrate into the inner ear tissue. In the cochlea, a number of MSCs formed cell masses on the surface of the scala timpani, where the majority of the surrounding tissue is bone tissue, suggesting that these MSCs did not invade the cochlear tissue. In the scala vestibuli, a small number of MSCs were also found attached to the surface of the bone and the Reissner membrane. However, in the apical part of the lateral wall, a number of MSCs were observed within the tissue, suggesting that MSCs had successfully invaded the lateral wall from the perilymph. This area may be an optimum site for MSC invasion. Furthermore, we performed DNA microarray analysis of the cochlear lateral wall RNAs in 3NP-treated rats and found a significant increase in the expression of the small inducible cytokine A2 gene encoding monocyte chemoattractant protein 1 (MCP1), which has been reported as a chemokine that induces migration of neural stem cells[24]. This may suggests that the MSC migration to the injured area of the lateral wall in this study may also be induced by chemokines because most MSCs were obsereved in the lateral wall in basal turn which had a prominent damage, but not in the apical turn.

Conclusion

Bone marrow MSCs have greater advantages for clinical use in human subjects than other multipotential stem cells, such as embryonic stem cells, because MSCs can be collected from the patient's own bone marrow for an autologous transplantation with little physical risk, no rejection risk, and few ethical problems. In the present transplantation, many MSCs were confirmed to have invaded the lateral wall and to have contributed to recovery of hearing loss despite transplantation between different rat strains. Therefore, we expect that autologous transplantation of bone marrow MSCs would be even more effective in treating hearing loss caused by injuries to the cochlear fibrocytes. In addition, significant improvement of hearing by MSC transplantation between different rat strains indicates a possibility of allogenic transplant. Even temporary effects by allogenic transplant may cause difference in the final outcome of hearing recovery by promoting regeneration or viability of host fibrocytes during acute period of injury.

Cell therapy targeting regeneration of the cochlear fibrocytes may therefore be a powerful strategy to cure sensorineural hearing loss that cannot be reversed by current therapies.

Acknowledgments

Most of the works had been done in National Institute of Sensory Organ, Japan (NISO). Special thanks for all the members of Laboratory of Auditory Disorders, NISO.

References

1) Hoya N, et al.: A novel animal model of acute cochlear mitochondrial dysfunction. Neuroreport, 15: 1597-1600, 2004.
2) Okamoto Y, et al.: Permanent threshold shift caused by acute cochlear mitochondrial dysfunction is primarily mediated by degeneration of the lateral wall of the cochlea. Audiol. Neurootol., 10: 220-233, 2005.
3) Kamiya K, et al.: Mesenchymal stem cell transplantation accelerates hearing recovery through the repair of injured cochlear fibrocytes. Am J Pathol, 171: 214-226, 2007.
4) Wangemann P: K+ cycling and the endocochlear potential. Hear. Res., 165: 1-9, 2002.
5) Weber PC et al.: Potassium recycling pathways in the human cochlea. Laryngoscope, 111: 1156-1165, 2001.
6) Delprat B et al.: Deafness and Cochlear Fibrocyte Alterations in Mice Deficient for the Inner Ear Protein Otospiralin. Mol. Cell. Biol., 25: 847-853, 2005.
7) Kikuchi T, et al.: Gap junctions in the rat cochlea: immunohistochemical and ultrastructural analysis. Anat Embryol. (Berl), 191: 101-118, 1995.
8) Spicer SS, Schulte, BA: The fine structure of spiral ligament cells relates to ion return to the stria

and varies with place-frequency. Hear. Res., 100: 80-100, 1996.

9) Minowa O, et al.: Altered cochlear fibrocytes in a mouse model of DFN3 nonsyndromic deafness. Science, 285: 1408-1411, 1999.

10) Xia AP et al.: Late-onset hearing loss in a mouse model of DFN3 non-syndromic deafness: morphologic and immunohistochemical analyses. Hear. Res., 166: 150-158, 2002.

11) Spicer SS, Schulte, BA: Spiral ligament pathology in quiet-aged gerbils. Hear. Res., 172: 172-185, 2002.

12) Hequembourg S, Liberman, MC: Spiral ligament pathology: a major aspect of age-related cochlear degeneration in C57BL/6 mice. J. Assoc. Res. Otolaryngol., 2: 118-129, 2001.

13) Wu T, Marcus, DC: Age-related changes in cochlear endolymphatic potassium and potential in CD-1 and CBA/CaJ mice. J Assoc. Res. Otolaryngol., 4: 353-362, 2003.

14) Kelsell DP, et al.: Connexin 26 mutations in hereditary non-syndromic sensorineural deafness. Nature, 387: 80-83, 1997.

15) del Castillo I, et al.: A deletion involving the connexin 30 gene in nonsyndromic hearing impairment. N. Engl. J Med., 346: 243-249, 2002.

16) Alston TA, et al.: 3-Nitropropionate, the toxic substance of Indigofera, is a suicide inactivator of succinate dehydrogenase. Proc. Natl. Acad. Sci. U S A, 74: 3767-3771, 1977.

17) Coles CJ, et al.: Inactivation of succinate dehydrogenase by 3-nitropropionate. J. Biol. Chem., 254: 5161-5167, 1979.

18) Brouillet E, et al.: Chronic mitochondrial energy impairment produces selective striatal degeneration and abnormal choreiform movements in primates. Proc. Natl. Acad. Sci. U S A, 92: 7105-7109, 1995.

19) Hamilton BF, Gould, DH: Nature and distribution of brain lesions in rats intoxicated with 3-nitropropionic acid: a type of hypoxic (energy deficient) brain damage. Acta Neuropathol. (Berl), 72: 286-297, 1987.

20) Pittenger MF, et al.: Multilineage potential of adult human mesenchymal stem cells. Science, 284: 143-147, 1999.

21) Liechty KW, et al.: Human mesenchymal stem cells engraft and demonstrate site-specific differentiation after in utero transplantation in sheep. Nat. Med., 6: 1282-1286, 2000.

22) Jiang Y, et al.: Pluripotency of mesenchymal stem cells derived from adult marrow. Nature, 418: 41-49, 2002.

23) Lang H, et al.: Contribution of bone marrow hematopoietic stem cells to adult mouse inner ear: mesenchymal cells and fibrocytes. J Comp Neurol, 496: 187-201, 2006.

24) Widera D, et al.: MCP-1 induces migration of adult neural stem cells. Eur. J. Cell Biol., 83: 381-387, 2004.

論文受付　21年5月18日
論文受理　21年5月18日

別刷請求先：〒171-0021　東京都文京区本郷2丁目1－1
順天堂大学医学部耳鼻咽喉科学教室　神谷　和作

Neuroscience 156 (2008) 1039–1047

POSTNATAL DEVELOPMENT OF THE ORGAN OF CORTI IN DOMINANT-NEGATIVE *GJB2* TRANSGENIC MICE

A. NOSHITA,[a] T. IZUKA,[a] H.-O. OKAMURA,[a] A. MINEKAWA,[a] K. KOJIMA,[b] M. FURUKAWA,[a] T. KUSUNOKI[a] AND K. IKEDA[a]*

[a]*Department of Otorhinolaryngology, Juntendo University School of Medicine, Hongo 2-1-1, Bunkyo-ku, Tokyo 113-8431, Japan*

[b]*Department of Otorhinolaryngology–Head and Neck Surgery, Kyoto University, Graduate School of Medicine, Japan*

Abstract—Hereditary hearing loss is one of the most prevalent inherited human birth defects, affecting one in 2000. A strikingly high proportion (50%) of congenital bilateral non-syndromic sensorineural deafness cases have been linked to mutations in the *GJB2* coding for the connexin26. It has been hypothesized that gap junctions in the cochlea, especially connexin26, provide an intercellular passage by which K^+ are transported to maintain high levels of the endocochlear potential essential for sensory hair cell excitation. We previously reported the generation of a mouse model carrying human connexin26 with R75W mutation (R75W+ mice). The present study attempted to evaluate postnatal development of the organ of Corti in the R75W+ mice. R75W+ mice have never shown auditory brainstem response waveforms throughout postnatal development, indicating the disturbance of auditory organ development. Histological observations at postnatal days (P) 5–14 were characterized by (i) absence of tunnel of Corti, Nuel's space, or spaces surrounding the outer hair cells, (ii) significantly small numbers of microtubules in inner pillar cells, (iii) shortening of height of the organ of Corti, and (iv) increase of the cross-sectional area of the cells of the organ of Corti. Thus, morphological observations confirmed that a dominant-negative *Gjb2* mutation showed incomplete development of the cochlear supporting cells. On the other hand, the development of the sensory hair cells, at least from P5 to P12, was not affected. The present study suggests that *Gjb2* is indispensable in the postnatal development of the organ of Corti and normal hearing. © 2008 IBRO. Published by Elsevier Ltd. All rights reserved.

Key words: hereditary hearing loss, mouse, organ of Corti, *Gjb2*.

Hereditary deafness affects about one in 2000 children and mutations in the connexin26 (Cx26) gene (*GJB2*) are the most common genetic cause of congenital bilateral non-syndromic sensorineural hearing loss. It has been hypothesized that gap junctions in the cochlea, especially Cx26, provide an intercellular passage by which K^+ are transported to maintain high levels of the endocochlear potential (EP), which is essential for sensory hair cell excitation. However, the pathogenesis of deafness remains unresolved because the electrophysiological and histological examination that can be carried out in humans is limited and partly because *Gjb2* deficient mice were embryonic lethal (Gabriel et al., 1998). We previously reported on transgenic mice (Tg) carrying human Cx26 with a R75W mutation that was identified in a deaf family with autosomal dominant negative inheritance. Although the EP remained within a normal range, the auditory brainstem response (ABR) revealed that the mice at postnatal day 14 (P14) showed severe to profound hearing loss. The tunnel of Corti was not detected and the shapes of outer hair cells (OHCs) were peculiar in the Tg mice at P14. These results suggested that the *Gjb2* mutation primarily disturbs homeostasis of cortilymph, an extracellular space surrounding the sensory hair cells, due to impaired potassium ion transport by supporting cells, secondarily resulting in degeneration of the organ of Corti, rather than affecting endolymph homeostasis in mice (Kudo at al., 2003).

Gap junctions are believed to be important for maturation and differentiation of developing tissues (Elias et al., 2007). Developmental expression of Cx26 in the mouse cochlea started in the inner and outer sulcus cells on the 18th day of gestation. At birth, immunolabeling for Cx26 was observed over the supporting cells of the inner hair cells (IHCs) and the mesenchymal components of the stria vascularis (Frenz and Van de Water, 2000). In contrast, Cx26 was not detected in the supporting cells in the organ of Corti before P3. Not until P8 was Cx26 immunoreactivity detected in almost all supporting cells in the organ of Corti (Zhang et al., 2005). Thus, evaluation of the postnatal development of *Gjb2* Tg mouse cochlea is required to obtain a better and accurate understanding of the molecular mechanism mediated by *Gjb2* mutation.

The present study was designed to evaluate the organ of Corti in the R75W+ mice compared with that of non-Tg mice from P5 to P14.

EXPERIMENTAL PROCEDURES

Animals and anesthesia

All mice used throughout this study were obtained from breeding colony with R75W+ mice (Kudo et al., 2003) and maintained at Institute for Animal Reproduction (Ibaraki, Japan). R75W+ mice were maintained on a mixed C57BL/6 background and intercrossed to generate R75W+ animals. The animals were genotyped using DNA obtained from tail clips and amplified with the

*Corresponding author. Tel: +81-3-5802-1094; fax: +81-3-5689-0547.
E-mail address: ike@med.juntendo.ac.jp (K. Ikeda).

Abbreviations: ABR, auditory brainstem response; Cx26, connexin26; DC, Deiter's cell; EDTA, ethylenediaminetetraacetic acid; EP, endocochlear potential; FGFR3, fibroblast growth factor receptor 3; GA, glutaraldehyde; *GJB2*, connexin26 gene; H-E, hematoxylin and eosin; IHC, inner hair cell; IPC, inner pillar cell; OHC, outer hair cell; OPC, outer pillar cell; P, postnatal day; PB, phosphate buffer; PBS, phosphate-buffered saline; PFA, paraformaldehyde; TEM, transmission electron microscopy; Tg, transgenic.

doi:10.1016/j.neuroscience.2008.08.027

Tissue PCR Kit (Sigma, St. Louis, MO, USA). All experiment protocols were approved by the Institutional Animal Care and Use Committee at Juntendo University, and were conducted in accordance with the US National Institutes of Health Guidelines for the Care and Use of Laboratory Animals. We minimized number of animals used and their suffering. Animals were deeply anesthetized with an i.p. injection of ketamine (100 mg/kg) and xylazine (10 mg/kg) in both ABR measurements and histological examinations.

ABR

All electrophysiological examinations were performed within an acoustically and electrically insulated and grounded test room. Mice ranging in age from P10 to P14 were studied. For ABR measurement, stainless-steel needle electrodes were placed at the vertex and ventrolateral to the left and right ears. The ABR was measured using waveform storing and stimulus control of Scope software of Power Laboratory system (model PowerLab4/25, AD Instruments, Castle Hill, Australia), and electroencephalogram recording was made with an extracellular amplifier AC PreAmplifier (model P-55, Astro-Med, West Warwick, RI, USA). Acoustic stimuli were delivered to the mice through a coupler type speaker (model: ES1spc, Bio Research Center, Nagoya, Japan). The threshold was determined for frequencies of 12, 24, 36, and 48 kHz from a set of responses at varying intensities with 5 dB intervals and electrical signals were averaged at 512 repetitions. If the hearing threshold was over 95 dB, it was determined as 100 dB.

Light microscopy

The animals were deeply anesthetized and perfused intracardially with 0.01 M phosphate-buffered saline (PBS; pH 7.2), followed by 4% paraformaldehyde (PFA; pH 7.4) in 0.1 M phosphate buffer (PB; pH 7.4). The mice were decapitated and their cochleae dissected out under a microscope and placed in the same fixative at room temperature for overnight. Cochlear specimens were then placed into 0.12 M EDTA (pH 7.0) in PBS for decalcification for a week, dehydrated and embedded in paraffin. Serial sections (6 μm) were stained with hematoxylin and eosin (H-E) staining.

Transmission electron microscopy (TEM)

The animals were deeply anesthetized and perfused intracardially with 0.01 M PBS, followed by 4% PFA and 2% glutaraldehyde (GA) in 0.1 M PB. The cochleae were opened and flushed with buffered 4% PFA and 2% GA and fixed for 2 h at room temperature. After washing, the specimens were post-fixed 1.5 h in 2% OsO_4 in 0.1 M PB, then dehydrated through graded ethanols and embedded in Epon. The samples were cut (1 μm), stained with uranyl acetate and lead citrate, and examined by electron microscopy (H-7100, Hitachi, Tokyo, Japan).

In order to observe microtubules of inner pillar cell (IPC), the mice at the age of P12 were selected. Cochleae were perfused *in situ* with 2.5% GA in 0.1 M PB (pH 7.4) containing 2% tannic acid through the round window, dissected and immersed in the same fixative for 2 h at room temperature. Post-fixation, dehydration and embedding were performed as described above. Ultrathin sections, 60 nm thick, were cut in cross-section.

Immunohistochemistry

The cochleae were removed after cardiac perfusion with 4% PFA, placed in the same fixative at room temperature for an hour, decalcified with 0.12 M EDTA at 4 °C overnight, cryoprotected in 30% sucrose, embedded in OCT, and 10-μm-thick-sections were collected. Sections were washed in several changes of 0.01 M PBS, blocked with 0.3% Triton X-100 in 0.01 M PBS for 30 min, and then incubated overnight at 4 °C with primary antibody diluted in 0.01 M PBS+0.3% Triton X-100. The following day, the tissues were rinsed with 0.01 M PBS, incubated for 6 h at 4 °C with a fluorescent-conjugated secondary antibody, rinsed with 0.01 M PBS, and then mounted in Vectashield containing DAPI (Vector Laboratories, Burlingame, CA, USA). The following primary antibodies were used: rabbit polyclonal antibodies to rabbit polyclonal antibodies to fibroblast growth factor receptor 3 (FGFR3) (1:200; Santa Cruz Biotechnology, Santa Cruz, CA, USA), rabbit polyclonal antibodies to $p27^{Kip1}$ (1:200; Lab Vision, Fremont, CA,

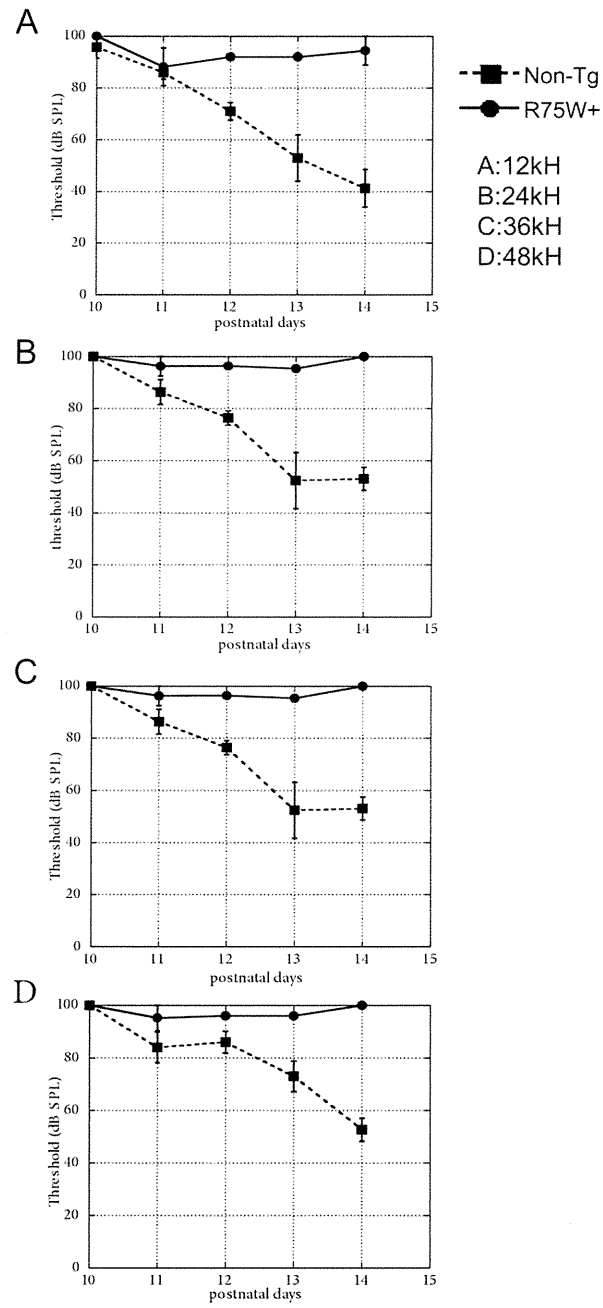

Fig. 1. Developmental change of the threshold levels of ABR of non-Tg and R75W+ mice at 12 kHz (A), 24 kHz (B), 36 kHz (C) and 48 kHz (D). The onset of hearing in non-Tg mice appears at P11, and ABR thresholds achieve adult level (dotted lines in A–D). ABR of R75W+ mice at P11 shows severe to profound deafness at overall sound pressure level (solid lines in A–D).

USA) and MyosinVIIa (1:500; Proteus Bio Sciences, CA, USA). Secondary antibodies used were Alexa-Fluor donkey anti-rabbit (1:500; Molecular Probes, Eugene, OR, USA). Images of sections were captured on a Zeiss Axioplan2 microscope using an AxioCam HRc CCD camera and Axio Vision Rel.4.2 software.

Quantification and statistical analysis

The number of microtubules of the IPC in 50 fields randomly selected was counted at magnifications of ×10,000, and was compared between R75W+ and non-Tg mice. The results were expressed as mean±S.D. Statistical significance was addressed by Student's *t*-test; $P<0.05$ was accepted as significant.

For measurement of the height and the cells area of the organ of Corti, midmodiolar section (1 μm) were counterstained with Toluidine Blue as described (Faddis et al., 1998). Digital light micrograph images of the organ of Corti were captured using following software. The height and the cell area of the organ of Corti were measured by using NIS Elements-D (Nikon, Tokyo, Japan). Two animals from each age group were analyzed.

RESULTS

The different findings were observed by ABR measurements in a group of R75W+ and non-Tg mice at the stage of hearing development (Fig. 1). The onset of hearing in non-Tg mice was recognized at P11 as previously described (Anniko, 1983), and ABR thresholds almost reached the adult level by P14. In contrast, R75W+ mice have never showed ABR waveforms throughout postnatal development, indicating the disturbance of auditory organ development. The ABR thresholds in R75W+ mice exceeded 95 dB, which is comparable to profound deafness observed in human congenital deafness due to *GJB2* mutations.

Histological examinations of the cochleae with H-E staining revealed no obvious changes of Reissner's membrane, stria vascularis, spiral ligament, and spiral ganglion cells in the mutant mice (Fig. 2). On the other hand, a

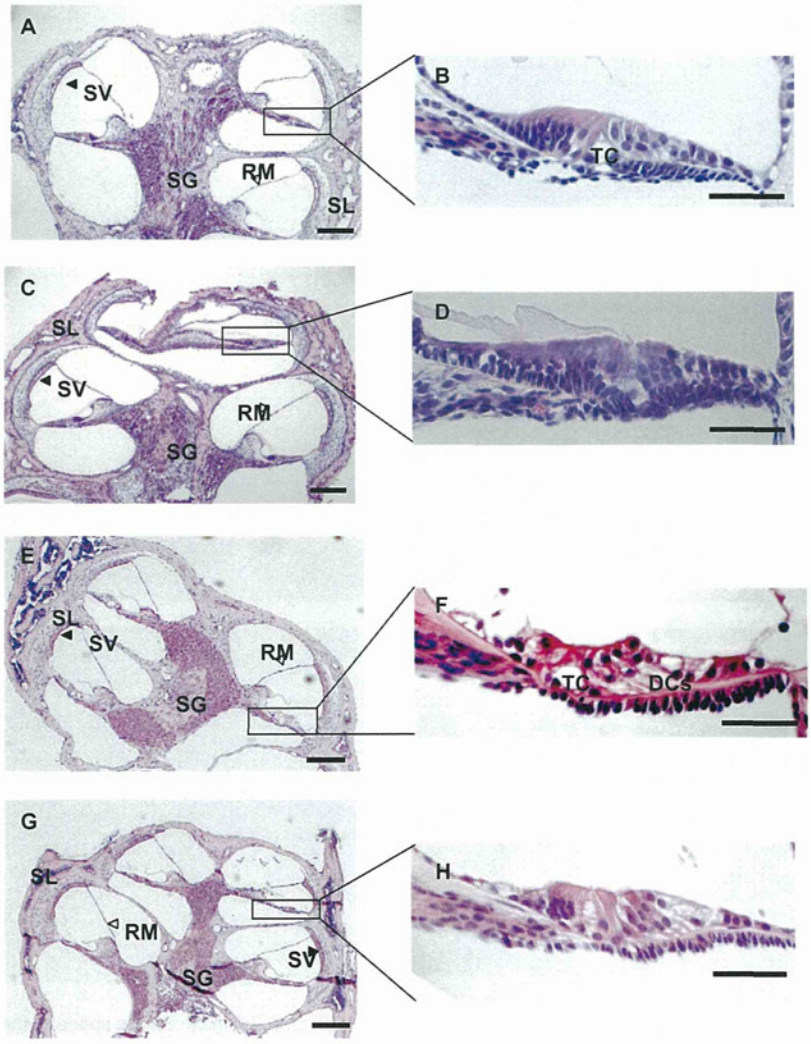

Fig. 2. Light microscopic findings of the cochlea. H-E staining presents defective changes in the organ of Corti obtained from animals at P8 (A, B) and P12 (E, F) of non-Tg mice and at P8 (C, D) and P12 (G, H) of R75W+ mice. Midmodiolar section was counterstained with H-E staining. No obvious changes are observed in RM; SV, SL, or SG (A, B, E, F). At P8 before the onset of hearing, tunnel of Corti is detected in non-Tg mice (B), but not in R75W+ mice (D). At P12, the DCs sit beneath the OHCs and Nuel's spaces are detected in non-Tg mice (F), but not in R75W+ mice (H). Abbreviations used: RM, Reissner's membrane; SV, stria vascularis; SL, spiral ligament; SG, spiral ganglion cells; TC, tunnel of Corti. Scale bar=100 μm (A–D); 50 μm (E–H).

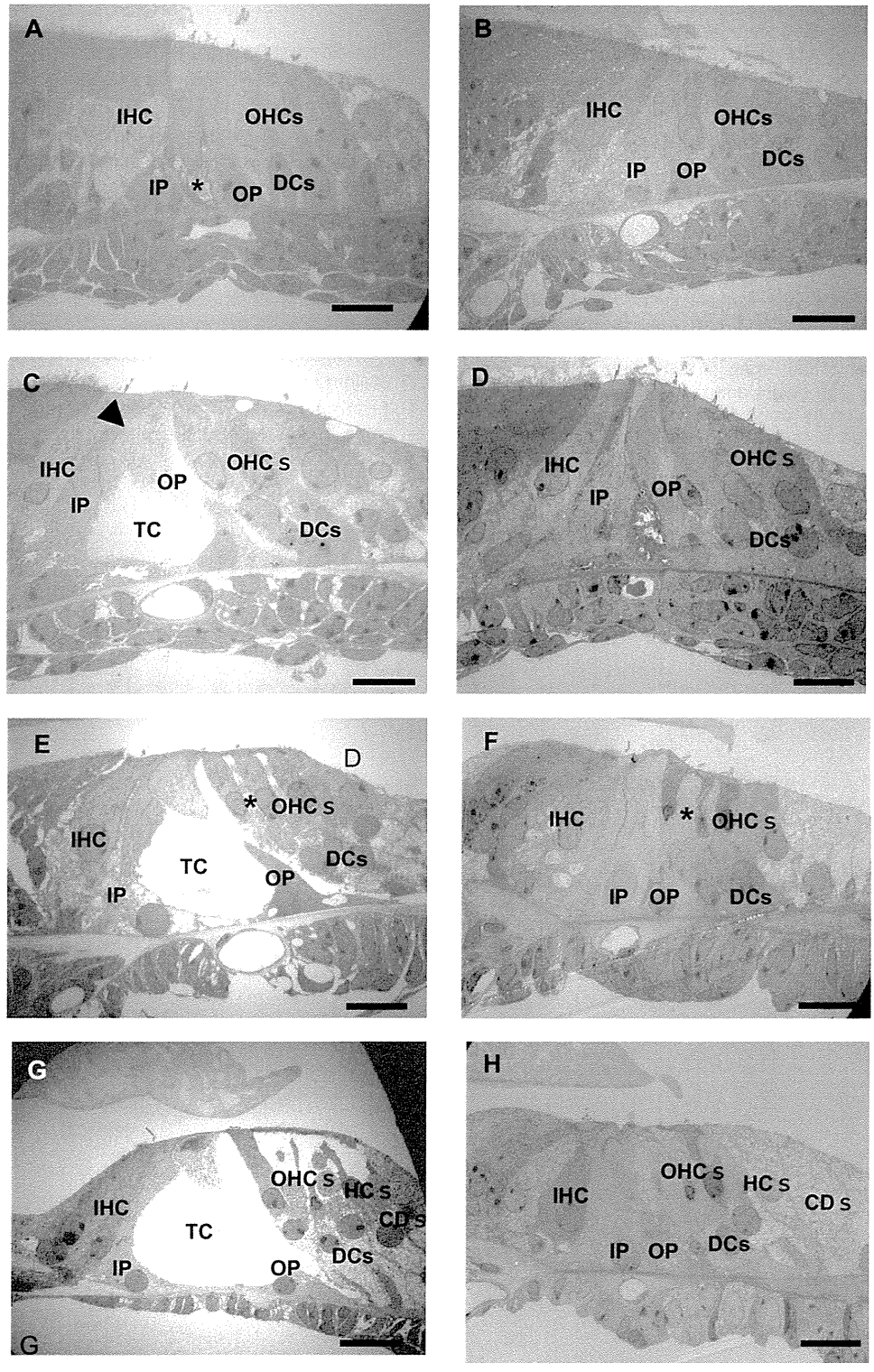

Fig. 3. Transmission electron micrographs of non-Tg (A, C, E, G) and R75W+ (B, D, F, H) mice. Future space of the tunnel of Corti (asterisk) starts to be formed in non-Tg mice (A), but is not detected in R75W+ mice (B) at P5. At P8, the open space between the IPCs and OPCs below their connection at a tight junction exceeds that of non-Tg mice (arrowhead in C). The TC is insufficient to be created in R75W+ mice (D). At P10, Nuel's space starts to be formed in non-Tg (asterisk in E) but not in R75W+ mice (asterisk in F). At P12, an adult-like configuration of the organ of Corti is created in non-Tg mice (G). The cell cytoplasm of supporting cells is enlarged in R75W+ mice (H). OHCs in R75W+ mice are squeezed by the surrounding DCs (F, H). Scale bar=10 μm. Abbreviations used: TC, tunnel of Corti; IP, inner pillar cell; OP, outer pillar cell; HC, Hensen cells; CDs, Claudius cells.

remarkable change of the collapse was recognized in the organ of Corti at least from P10 in the light microscopy (data not shown).

Ultrastructural analysis was performed to evaluate the fine structure of the organ of Corti in the late developmental stage. An analysis by TEM demonstrated further details of histological alterations in the organ of Corti (Fig. 3). The opening of tunnel of Corti between the IPC and outer pillar cell (OPC) were seen at P5 in non-Tg mice (Fig. 3A). In contrast, no spaces within IPC and OPC were apparent at P5 onward in R75W+ mice (Fig. 3B). No obvious structural change was observed in the other cells of the organ of Corti at P5. At P8 in both non-Tg and R75W+ mice, during expansion of tunnel of Corti, the pillar cell bodies were distinguished from the surrounding cells (Fig. 3C, 3D). At P10 in non-Tg mice, extensive Nuel's space opening occurred (Fig. 3E). In contrast, the future Nuel's spaces were occupied by bulky processes of Deiter's cells (DCs) in R75W+ mice (Fig. 3F). At P12, non-Tg mice approached a well-matured configuration (Fig. 3G). Supporting cells of R75W+mice (Fig. 3H) tended to be grossly enlarged as compared with non-Tg. In the R75W+ mice, the IHC from P5 to P12 and the OHC from P5 to P8 had a relatively normal shape. Numerous mitochondria were located along the lateral membrane of the OHCs which was lined by a thick layer of subsurface cisternae (data not shown). However, DCs surrounded and compressed the OHCs at P10–12 (Fig. 3F, 3H).

Both IPCs and OPCs showed a nearly mature appearance, in which abundant microtubules were formed parallel array in non-Tg mice (Fig. 4A) whereas microtubules of the IPCs were poorly formed and hypoplasia occurred in R75W+ mice (Fig. 4B). Actually, the average number of microtubules of the cross-section of the IPCs at P12 in R75W+ mice ($4.4\pm3.3/100\ \mu m^2$) was significantly reduced (Fig. 4D) as compared with that of non-Tg mice ($26.9\pm25.6/100\ \mu m^2$) (Fig. 4C).

Quantitative data describing peak height and cell areas of the organ of Corti also showed the differences between non-Tg and R75W+ mice (Fig. 5). The height of the organ of Corti in non-Tg mice showed an increase with the development of the organ of Corti as described previously (Souter et al., 1997). In contrast, the height remained unchanged presumably due to collapse of tunnel of Corti in R75W+ mice (Fig. 5A). The cell area of the organ of Corti showed no difference between non-Tg and R75W+ mice at P5, both of which increased rapidly until P8. Although the increase of cell area appeared slowly after the formation of tunnel of Corti and Nuel's space at P8 in non-Tg mice, the area increased from P10 to P12 in R75W+ mice (Fig. 5B). The increase of the cell area from P10–12 recognized in R75W+ mice is assumed to be brought about by the enlarged supporting cells. Thus, the dominant-negative mutant of *Gjb2* disrupted postnatal development of supporting cells.

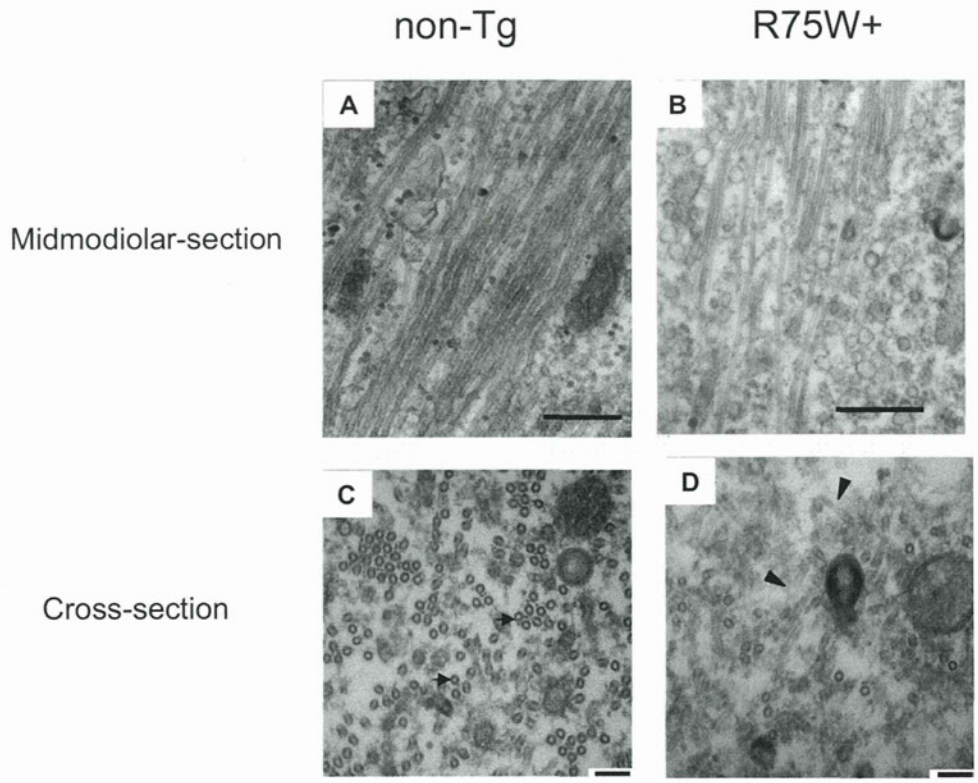

Fig. 4. The microtubules of the midmodiolar- (A, B) and cross-sections (C, D) of the IPC at P12. The microtubules are rich in the IPC in non-Tg mice (arrows in A). The microtubules of the IPC are poorly formed and hypoplasia in R75W+ mice (arrows in B). Round-shaped microtubules with cross-sections are abundant in non-Tg mice (arrows in C). (D) The number of microtubules is reduced and the tangled microtubules (arrows in D) are prominent in R75W+ mice. Scale bar=500 nm (A, B); 1 μm (C, D).

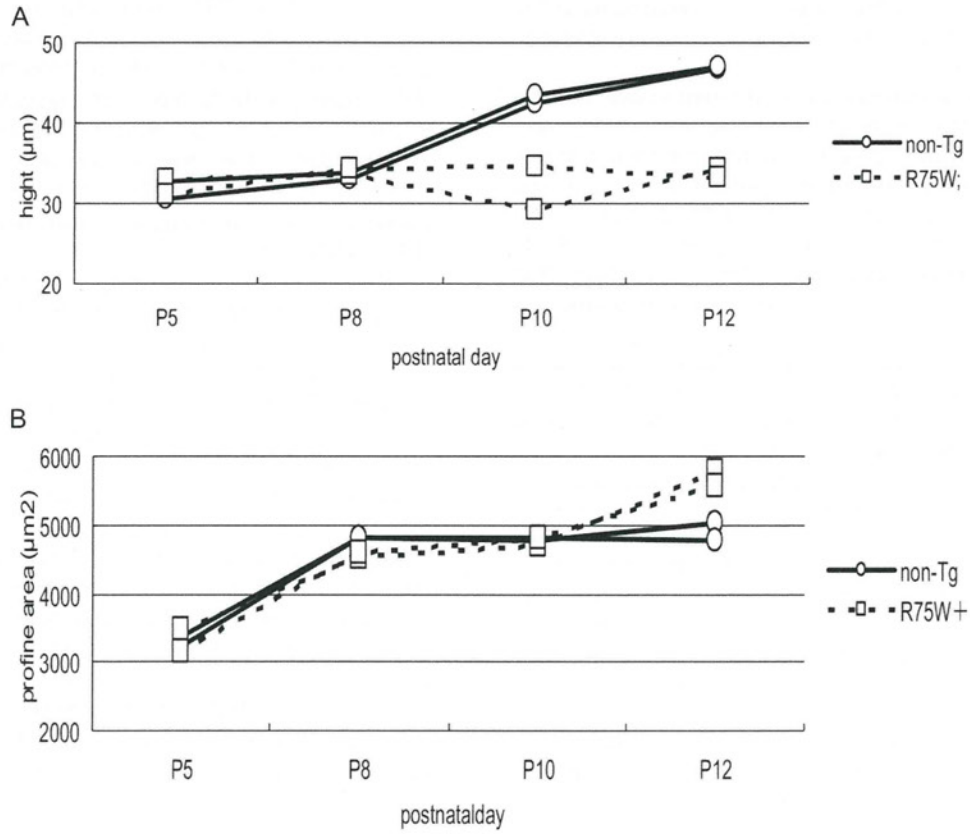

Fig. 5. The height of (A) and cell area (B) of the organ of Corti in individual mice of non-Tg (n=2) and R75W+ (n=2). R75W+ mice show the reduction of the height of the organ of Corti from P10 as compared with non-Tg mice (A). At P12, the profile area of the organ of Corti of R75W+ mice is greater than that of non-Tg mice (B).

Since it is possible that the *Gjb2* gene affects the known genes to determine or differentiate regarding hair or supporting cells, the protein expression of FGFR3 and $p27^{Kip1}$ for supporting cell markers, and MyosinVIIa for a hair cell marker were examined at P12. Similar results regarding the immunolabeling of the cochlear section for the tested antibodies were obtained in both R75W+ and non-Tg mice (Fig. 6).

DISCUSSION

The present study demonstrated that ABR have never been recognized in the postnatal stage of R75W+ mice from P5 to P14. On the other hand, non-Tg mice showed the onset of ABR at P11, which approached near maturity until P14. These findings may be explained by the supposition that the cochlear function does not reach maturation in a dominant-negative mutation of *Gjb2*.

The characteristic changes of ultrastructures observed in the developing non-sensory cells of the organ of Corti include: i) absence of tunnel of Corti, Nuel's space, or spaces surrounding the OHCs; ii) significant small numbers of microtubules in IPCs; iii) shortening of height of the organ of Corti; and iv) increase of the midmodiolar-sectional area of the cells of the organ of Corti. Thus, morphological observations confirmed that a dominant-negative *Gjb2* mutation showed incomplete development of the cochlear supporting cells. On the other hand, the development of the sensory hair cells at least from P5 to P12 was not affected, which is not surprising since the sensory hair cells do not express Cx26 throughout development. In fact, *MyosinVIIa*, a major gene identified in hair cells was expressed in the developing hair cells of R75W+ mice.

Our dominant-negative *Gjb2* mutant mice showed a phenotype apparently different from that of a target disruption of *Gjb2* (Cohen-Salmon et al., 2002), in which the inner ear normally developed up to P14 followed by the degeneration of the cochlear epithelial networks and sensory hair cells. Furthermore, our preliminary study (Ikeda et al., 2004) in a creation of a conditional knockout of *Gjb2* using the promoter different from that of Cohen-Salmon et al. (2002) showed comparable findings to the present dominant-negative *Gjb2* mutant. Both animal models of *Gjb2*-based hereditary deafness developed by us strongly indicate that *Gjb2* is indispensable throughout the postnatal development of the organ of Corti, especially from P5 to maturation.

The development of pillar cells and the formation of a normal tunnel of Corti are required for normal hearing (Colvin et al., 1996). The factors that regulate pillar cells development are *Fgfr3* (Mueller et al., 2002). The mice homozygous for a targeted disruption of *Fgfr3* had striking inner ear defects and were deaf. In the organ of Corti of

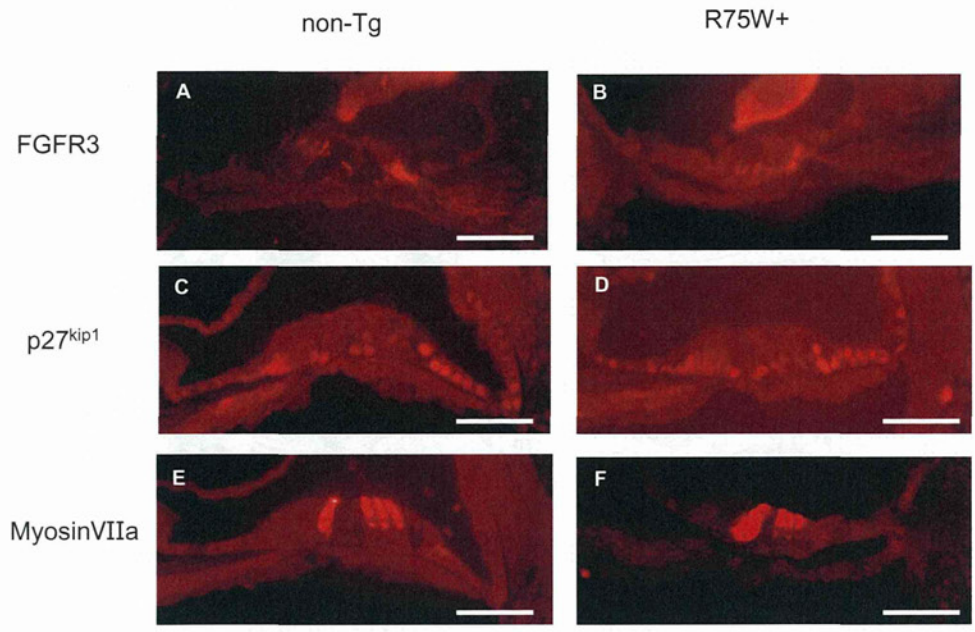

Fig. 6. Immunohistochemical analysis of the inner ear. Expressions of the FGFR3 are specifically localized in pillar cells in both non-Tg (A) and R75W+ (B). Expressions of the $p27^{Kip1}$ are labeled in nucleus of supporting cells in both non-Tg (C) and R75W+ (D). The inner and OHCs are labeled with MyosinVIIa in both non-Tg (E) and R75W+ (F). Scale bar=100 μm.

Fgfr3 deficient mice, differentiated pillar cells and the tunnel space were completely absent and ABR showed no response at 100 dB SPL (Colvin at al., 1996), which is interesting as it is similar to the observations of our R75W+ mice. It is possible that the cochlear *Gjb2* regulates differentiation genes of the supporting cells at the transcriptional or translational level. However, the expression of *Fgfr3* and $p27^{Kip1}$ proteins in the R75W+ mouse cochlea was equivalent to those of non-Tg mouse, which seems to negate the involvement of *Fgfr3* and $p27^{Kip1}$ genes to the disrupted differentiation of pillar cells and other supporting cells. It is possible to cause the effect similar to *Fgfr3* disruption by mediating its upstream and downstream pathways. Further studies are required to obtain a better understanding of the relevance of the *Fgfr3* pathway. The mutant mice of thyroid hormonal receptors were reported to have delayed postnatal development of the organ of Corti (Rusch et al., 2001). The phenotype of thyroid hormonal receptor mutants is similar to our phenotype with respect to the unopened tunnel of Corti, but not to the formation of tectorial membrane or the development of EP. Although the typical distribution of prestin along the OHC lateral membrane was found to depend on the thyroid hormone receptor TRβ (Winter et al., 2006), prestin was normally expressed in our Tg mice (our unpublished observations). These findings suggest that thyroid hormone is not related to the phenotype of the *Gjb2* dominant-negative mutation.

The results presented here demonstrate a significant reduction of the number of microtubules in the pillar cells in R75W+ mice, which presumably causes absence of the tunnel and incomplete height of the organ of Corti. The microtubules in the pillar cells appear to be unique to mammalian cochlea with respect to the aspect of a strong and rigid cytoskeleton for maintenance of cell shape and effective transduction of vibratory stimuli on the sensory epithelium (Saito and Hama, 1982; Slepecky et al., 1995). The disturbed formation of microtubules in DCs, which were not evaluated in the present study, is expected to take a place similar to pillar cells and may lead to failure to form Nuel's space as well as a lack of DC cup surrounding the hair cells and the nerve ending.

Morphometric analysis of cross-sectional areas of the cells of the organ of Corti suggests the reduction of cell volume whereas extracellular spaces such as tunnel of Corti, Nuel's space, and spaces surrounding OHCs were apparently diminished under the TEM observation. Inhibitory effects of channels, transporters, and fluid secretion are suspected to be mediated by cell-signal molecules through the gap junctions (Beltramello et al., 2005; Lang et al., 2007; Piazza et al., 2007; Zhang et al., 2005; Zhao et al., 2005). K-Cl cotransporters encoded by Kcc3 and Kcc4 are selectively expressed in DCs from late postnatal development and are thought to regulate the cell volume and the ionic environment of cortilymph (Boettger et al., 2002, 2003). The mouse cochlea deleting Kcc3 or Kcc4 resemble the phenotype of our R75W+ mice, implying that the increase of sectional-area of the cells of the organ of Corti may involve dysfunction of K-Cl cotransport in the DCs of R75W+ mice. The progressive degeneration of hair cells observed in the adult R75W+ mice (Kudo et al., 2003) may be brought about by the changes in the ionic composition of the cortilymph surrounding the basolateral surface of the hair cells (Ben-Yosef et al., 2003).

Gap junction proteins in the cochlear supporting cells are hypothesized to allow rapid removal of K^+ away from the base of hair cells, resulting in recycling back to the endolymph (Kikuchi et al., 1995). In addition to the K^+

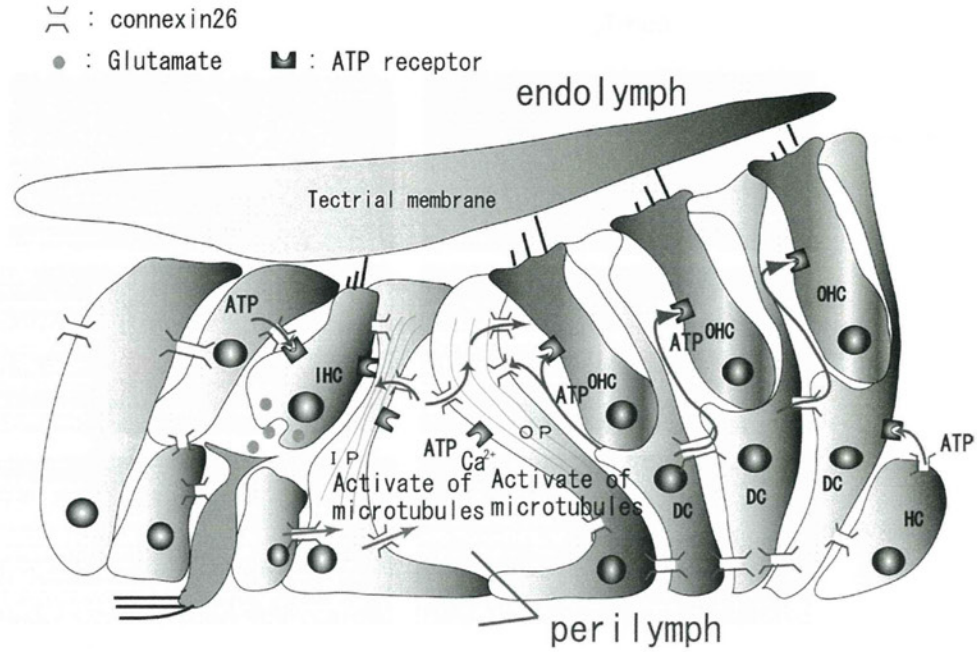

Fig. 7. Hypothesized schematic diagram of proposed intercellular signaling pathways between supporting cells and hair cells in the cochlea. ATP released from supporting cells via connexin hemichannels activates purinergic receptors on the hair cells or supporting cells in an autocrine and paracrine manner. Defective Cx26 is postulated to disrupt depolarization in the IHC and OHC, which may influence the glutamate release and the production of neurotrophic factors, respectively. Moreover, the failure of polymerization of the microtubules in the pillar cells may result from the disturbance of ATP release and/or intercellular signal transduction.

recycling theory, Ca^{2+} and anions such as inositol 1,4, 5-trisphosphate, ATP, and cAMP are mediated by gap junction proteins to act as cell-signaling and nutrient and energy molecules (Beltramello et al., 2005; Piazza et al., 2007; Zhang et al., 2005; Zhao et al., 2005). More currently, Tritsch et al. (2007) found that, in the postnatal immature cochlea, a transient structure known as Kölliker organ releases ATP through the hemichannels of its gap junctions, which binds to P2X receptors on the IHCs to cause depolarization and Ca^{2+} influx, mimicking the effect of sound. The resulting release of glutamate activates receptors on the afferent fibers, which is essential for the development of the auditory pathway. ATP is known to act as trophic factor, mitogen and potent neuromodulator (Fields and Burnstock, 2006; Nedergaard et al., 2003). Since supporting cells express ATP receptors (Dulon et al., 1993), the same scenario is likely to occur in an adapted form with the organ of Corti. The supporting cells may have an influence on maturation, cell volume and cell shape at least through the polymerization of microtubules by activated by ATP in an autocrine and paracrine manner (Zhao et al., 2005). We propose the hypothesis of an underlying mechanism to explain the prelingual deafness caused by *Gjb2* mutation (Fig. 7). Defective gap junction impairs the release of ATP and other factors related to cell-signaling and nutrient and energy molecules, resulting in the disturbance of normal postnatal development of the organ of Corti. Postnatal maturation of the various cochlear cells in the organ of Corti rapidly and synchronously progressed at P5 to P12 and may be regulated by intercellular signal transduction mediated by ions and biomodulators via the gap junction network derived from Cx26. Furthermore, a similar hypothesis may involve the postnatal development of the stria vascularis and spiral ligament because of the presence of purinergic receptors (Ikeda et al., 1995; Liu et al., 1995; Ogawa and Schacht, 1995) and the source of ATP (White et al., 1995; Suzuki et al., 1997).

CONCLUSION

In conclusion, the present findings strongly support that *Gjb2* is indispensable in the postnatal development of the organ of Corti and normal hearing.

Acknowledgments—This work was supported in part by research grant from the Ministry of Education, Science, and Culture of Japan (Nos. 16209050, 17659538, and 19659441) and Uehara Memorial Foundation.

REFERENCES

Anniko M (1983) Postnatal maturation of cochlear sensory hairs in the mouse. Anat Embyol (Berl) 166:355–368.

Beltramello M, Piazza V, Bukauskas FF, Pozzan T, Mammano F (2005) Impaired permeability to Ins(1,4,5)P3 in a mutant connexin underlies recessive hereditary deafness. Nat Cell Biol 2005 7:63–69.

Ben-Yosef T, Belyantseva IA, Saunders TL, Hughes ED, Kawamoto K, Van Itallie CM, Beyer LA, Halsey K, Gardner DJ, Wilcox ER, Rasmussen J, Anderson JM, Dolan DF, Forge A, Raphael Y, Camper SA, Friedman TB (2003) Claudin 14 knockout mice, a model for autosomal recessive deafness DFNB29, are deaf due to cochlear hair cell degeneration. Hum Mol Genet 12:2049–2061.

Boettger T, Hübner CA, Maier H, Rust MB, Beck FX, Jentsch TJ (2002) Deafness and renal tubular acidosis in mice lacking the K-Cl co-transporter Kcc4. Nature 416:874–878.

Boettger T, Rust MB, Maier H, Seidenbecher T, Schweizer M, Keating DJ, Faulhaber J, Ehmke H, Pfeffer C, Scheel O, Lemcke B, Horst J, Leuwer R, Pape HC, Völkl H, Hübner CA, Jentsch TJ (2003) Loss of K-Cl co-transporter KCC3 causes deafness, neurodegeneration and reduced seizure threshold. EMBO J 22:5422–5434.

Cohen-Salmon M, Ott T, Michel V, Hardelin JP, Perfettini I, Eybalin M, Wu T, Marcus DC, Wangemann P, Willecke K, Petit C (2002) Targeted ablation of connexin26 in the inner ear epithelial gap junction network causes hearing impairment and cell death. Curr Biol 12:1106–1111.

Colvin JS, Bohne BA, Harding GW, McEwen DG, Ornitz DM (1996) Skeletal overgrowth and deafness in mice lacking fibroblast growth factor receptor 3. Nat Genet 12:390–397.

Dulon D, Moataz R, Mollard P (1993) Characterization of Ca^{2+} signals generated by extracellular nucleotides in supporting cells of the organ of Corti. Cell Calcium 14:245–254.

Elias LA, Wang DD, Kriegstein AR (2007) Gap junction adhesion is necessary for radial migration in the neocortex. Nature 448: 901–907.

Faddis BT, Hughes RM, Miller JD (1998) Quantitative measures reflect degeneration, but not regeneration, in the deafness mouse organ of Corti. Hear Res 115:6–12.

Fields RD, Burnstock G (2006) Purinergic signaling in neuron-glia interactions. Nat Rev Neurosci 7:423–436.

Frenz CM, Van de Water TR (2000) Immunolocalization of connexin 26 in the developing mouse cochlea. Brain Res Rev 32:172–180.

Gabriel HD, Jung D, Butzler C, Temme A, Traub O, Winterhager E, Willecke K (1998) Transplacental uptake of glucose is decreased in embryonic lethal connexin26-deficient mice. J Cell Biol 140:1453–1461.

Ikeda K, Kudo T, Jin ZH, Gotoh S, Katori Y, Kikuchi T, Minowa O, Noda T (2004) Conditional gene targeting of *Gjb2* results in profound deafness due to maturation failure of the organ of Corti. 27th Midwinter research meeting, #762.

Ikeda K, Suzuki M, Furukawa M, Takasaka T (1995) Calcium mobilization and entry induced by extracellular ATP in the non-sensory epithelial cell of the cochlear lateral wall. Cell Calcium 18:89–99.

Kikuchi T, Kimura RS, Paul DL, Adams JC (1995) Gap junctions in the rat cochlea: immunohistochemical and ultrastructural analysis. Anat Embryol 191:101–118.

Kudo T, Kure S, Ikeda K, Xia AP, Katori Y, Suzuki M, Kojima K, Ichinohe A, Suzuki Y, Aoki Y, Kobayashi T, Matsubara Y (2003) Transgenic expression of a dominant-negative connexin26 causes degeneration of the organ of Corti and non-syndromic deafness. Hum Mol Genet 12:995–1004.

Lang F, Vallon V, Knipper M, Wangemann P (2007) Functional significance of channels and transporters expressed in the inner ear and kidney. Am J Physiol Cell Physiol 293:C1187–C1208.

Liu J, Kozakura K, Marcus DC (1995) Evidence for purinergic receptors in vestibular dark cell and strial marginal cell epithelia of the gerbil. Auditory Neurosci 1:331–340.

Mueller KL, Jacques BE, Kelly MW (2002) Fibroblast growth factor signaling regulates pillar cell development in the organ of. Corti J Neurosci 22:9368–9377.

Nedergaard M, Ransom B, Goldman SA (2003) New roles for astrocytes: redefining the functional architecture of the brain. Trends Neurosci 26:523–530.

Ogawa K, Schacht J (1995) P2y purinergic receptors coupled to phosphoinositide hydrolysis in tissues of the cochlear lateral wall. Neurorepor 6:1538–1540.

Piazza V, Ciubotaru CD, Gale JE, Mammano F (2007) Purinergic signalling and intercellular Ca^{2+} wave propagation in the organ of Corti. Cell Calcium 41:77–86.

Rusch A, Ng L, Goodyear R, Oliver D, Lisoukov I, Vennstrom B, Richardson G, Kelley MW, Forrest D (2001) Retardation of cochlear maturation and impaired hair cell function caused by deletion of all known thyroid hormone receptors. J Neurosci 21:9792–9800.

Saito K, Hama K (1982) Structural diversity of microtubules in the supporting cells of the sensory epithelium of guinea pig organ of Corti. J Electron Microsc 31:278–281.

Slepecky NB, Henderson CG, Saha C (1995) Post-translational modifications of tubulin suggest that dynamic microtubules are present in sensory cells and stable microtubules are present in supporting cells of the mammalian cochlea. Hear Res 91:136–147.

Souter M, Nevill G, Forge A (1997) Postnatal maturation of the organ of Corti in gerbils: morphology and physiological responses. J Comp Neurol 386:635–651.

Suzuki H, Ikeda K, Furukawa M, Takasaka T (1997) P2 purinoceptor of the globular substance in the otoconial membrane of the guinea pig inner ear. Am J Physiol 273:C1533–C1540.

Tritsch NX, Yi E, Gale JE, Glowatzki E, Bergles DE (2007) The origin of spontaneous activity in the developing auditory system. Nature 450:50–55.

White PN, Thorne PR, Housley GD, Mockett B, Billett TE, Burnstock G (1995) Quinacrine staining of marginal cells in the stria vascularis of the guinea-pig cochlea: a possible source of extracellular ATP? Hear Res 90:97–105.

Winter H, Braig C, Zimmermann U, Geisler HS, Fränzer JT, Weber T, Ley M, Engel J, Knirsch M, Bauer K, Christ S, Walsh EJ, McGee J, Köpschall I, Rohbock K, Knipper M (2006) Thyroid hormone receptors TRalpha1 and TRbeta differentially regulate gene expression of Kcnq4 and prestin during final differentiation of outer hair cells. J Cell Sci 119:2975–2984.

Zhang Y, Tang W, Ahmad S, Sipp JA, Chen P, Lin X (2005) Gap junction-mediated intercellular biochemical coupling in cochlear supporting cells is required for normal cochlear function. Proc Natl Acad Sci U S A 102:15201–15206.

Zhao HB, Yu N, Fleming CR (2005) Gap junctional hemichannel-mediated ATP release and hearing controls in the inner ear. Proc Natl Acad Sci U S A 102:18724–18729.

(Accepted 11 August 2008)
(Available online 22 August 2008)